Synthetic Generation of Radio Maps for Device-Free Passive Localization

Ahmed Eleryan and Mohamed Elsabagh*
Dept. of Computer and Systems Engineering
Faculty of Engineering
Alexandria University, Egypt
{ahmed.eleryan,mohamed.elsabagh}@alex.edu.eg

Moustafa Youssef
Dept. of Computer Science and Engineering
Egypt-Japan University of Science and Technology
Alexandria, Egypt
moustafa.youssef@ejust.edu.eg

***Abstract*—In this paper, we present the design, implementation, and evaluation of a system that automatically constructs accurate radio maps for device-free WLAN localization systems. The system is capable of generating deterministic and probabilistic radio maps for localization systems. Our system uses 3D ray tracing enhanced with the uniform theory of diffraction (UTD) to model the electric field behavior and the human shadowing effect. We present our system architecture and describe the details of its different components. We also propose an optional module, location-0 correction, that can significantly enhances the system accuracy and reduces its dependence on the 3D model details by using just one signal strength sample. Our experiments in a real testbed show that the predicted signal strength differs from the measurements by a maximum average absolute error of 2.77 dB achieving a maximum localization error of 3.13m and 2.84m for both the deterministic and probabilistic radio maps, respectively. In addition, the results show that our system is not sensitive to the 3D model details.**

I. Introduction

WLANs are installed primarily for providing wireless communications. However, recent research has shown that WLANs can be used in location determination in indoor environments, without using any extra hardware [1]–[3]. Acquiring the location information for a tracked entity unleashes the possibility of various context-aware applications including location-aware information retrieval, indoor direction finding, and intrusion detection.

There are two classes of WLAN location determination systems: device-based, e.g. [1], [2] and device-free, e.g. [3]–[5]. Device-based systems track the location of a WLAN-enabled device, such as a laptop or PDA. On the other hand, device-free systems do not require the entity being tracked to carry a device and depend on analyzing the effect of the tracked entity on the signal strength to estimate the entity's position. Device-free localization enables a wide set of new applications including intrusion detection, smart homes, and sensor-less sensing. Such systems are composed of a number of access points (APs) and monitoring points (MPs). The MPs, such as standard laptops and other wireless-enabled devices, monitor the strength of the APs signals and their positions are fixed.

* Mohamed Elsabagh is also with the Wireless Intelligent Networks Center, Nile University, Egypt. e-mail: mohamed.elsabagh@nileu.edu.eg

WiFi localization systems typically work in two phases [3]. First, an *offline* phase where the system collects signal strengths received from different streams at different selected locations in the area of interest, and tabulates them into a so-called *radio map* [1], [3]. Second, a location determination phase where the system uses the information stored in the *radio map* to estimate the user's location. Different location determination systems store different information in the radio map. In a *deterministic* radio map, e.g. [3], the system represents the signal strength received from each AP by a single value, while for a *probabilistic* radio map, e.g. [2], the radio map stores information about the distribution of the signal strength received from each AP.

The problem with existing methods is that they all depend on manual calibration, which is tedious and time consuming. Specifically, each time the layout of the environment is changed or different hardware is used, the whole process of location fingerprinting and radio map construction has to be repeated. Furthermore, the process of radio map construction gets more complicated in the device-free case when the number of tracked entities increases, since the radio map needs to take all location combinations into account. For example, for a radio map with l locations and a system that tracks up to n entities, the radio map needs to store information about $\binom{l}{n}$ possibilities. This emphasizes the need for a method to automatically construct the radio maps for an area of interest.

In this paper, we study the problem of generating radio maps for a given area of interest. We present a system that is unique in supporting automatic radio map generation for **device-free** localization systems. The method used combines ray tracing with the uniform theory of diffraction [6] to model both the RF propagation and human shadowing effect. Ray tracing approximates the electromagnetic waves as a set of discrete ray tubes that propagate through the area of interest and that undergo attenuation, reflection, transmission and diffraction due to the complexity of an indoor environment. Although ray tracing has been used before in site-specific radio propagation prediction and several tools have been developed, e.g. [7], [8], the main focus of such tools was the **radio coverage** problem, i.e., determining the coverage holes given the positions of the access points. In [9], a system for automatic radio map construction for device-based

localization systems was proposed. The system requires as an input a number of site-specific measurements and RSSI readings while global attenuation parameters are automatically estimated using simulated annealing search. In [10], given a blueprint of a building, RF receivers locations, and the received signal measurements, a localization system is proposed where backward ray tracing is used to predict the location of the RF signal emitters. Nevertheless, none of these systems account for the human shadowing effect on the RF signal nor they support device-free localization.

Different from all other systems, ***ours is unique*** in supporting automatic radio map generation for **device-free** localization. To our knowledge, it is the first system to consider radio map generation for device-free localization and the first to consider human effects in the process of radio map generation. Radio maps for **both** deterministic and probabilistic localization algorithms are supported. Our system has three main goals: (1) to automatically construct an accurate radio map for a site of interest, (2) to have efficient computations, and (3) to incur minimum overhead on the user.

The rest of the paper is organized as follows. Section II presents the details of our system. We evaluate the performance of the system in Section III. Finally, Section IV concludes the paper and gives directions for future work.

II. System Model

In this section, we describe our system architecture (Figure 1).

A. Input

The input to our system is the 3D model of the site of interest The 3D manipulation of the site model is done using the jMonkeyEngine (jME) which is a high performance open-source Java-based gaming engine.

Besides the 3D model, the user must provide the site-specific configuration. This includes the locations and antenna characteristics of the APs and MPs. The antenna characteristics include transmitting power, frequency, maximum gain and radiation pattern. The system comes with two pre-defined antenna radiation patterns: isotropic and half-wave dipole antenna. The user can also define a customized radiation pattern depending on the hardware used.

The system also comes with a built-in DB of the approximate values of the RF propagation properties of common building materials such as bricks and concrete. The user has the option of using this DB or providing customized values using the UI tool.

B. Ray Tracing Engine

The *Ray Tracing Engine* is the core of the system and is composed of three modules: the *Ray Launcher*, the *UTD Engine*, and the *Ray Receiver*.

The *Ray Launcher* samples the electromagnetic waves emitted from the the APs into a set of discrete ray tubes covering the area of interest uniformly and each having an associated electric field. In order to satisfy the conditions of uniformity specified in [11], the rays are emitted through the vertices of an icosahedron whose center is the AP. To achieve a better angular resolution, the face of the icosahedron is divided into smaller triangles using a tessellation frequency N [7].

The ray tubes propagate into the environment and undergo reflections, transmissions and diffractions. The *Ray Tracing Engine* handles the interactions of the ray tubes with the environment. After a specific number of interactions (the tracing depth), which is user-defined, a ray is ignored and is no further processed.

The *UTD Engine* handles the changes in the electric field associated with the ray tubes resulting from these interactions. These changes are modeled with Geometric Optics augmented with the Uniform Theory of Diffraction (UTD) [6].

The contribution of each tube in the final received signal strength at the MPs are found by the *Ray Receiver*. We used the reception sphere model [7], where a sphere is formed around the MP such that at most one ray from a wavefront intersects with the sphere.

C. Human Modeling

The construction of device-free radio maps requires modeling of human's body effect on the RF signals. At microwave frequencies and higher, the human body constitutes an impassable reflector for electromagnetic waves. That is, incident waves are reflected and diffracted off the body, along other interactions with the surrounding environment. Previous work in human modeling has shown a strong correlation between the RF characteristics of the human body and a metallic circular cylinder [12] in indoor radio channels. Therefore, we use a metallic cylinder to model the human body with radius 0.15m, and height 2m [12]. The field reflected off a cylindrical surface from an incident electric field is given by [6].

$$E^r(p) = E^i(Q_r) \cdot R_{s,h} \cdot A(s) \cdot e^{-jks^r} \quad (1)$$

Where:

- $E^i(Q_r)$ is the electric field incident to the cylinder at Q_r.
- $R_{s,h}$ are the soft and hard UTD reflection coefficients.
- $A(s)$ is the 3-D spreading factor of reflection.
- e^{-jks^r} is the phase shift of the reflected field.
- s^r is the distance between reflection point and observation point.

D. Device-Free Location-0 Correction

Due to the deviation of the 3D model from the actual environment, there is usually a constant offset between the measured and the predicted RSS (Section III-C1). One of the methods to make up for the effects of this deviation is to feed our system with a single RSS measured during the silence period (i.e. when the environment is free from humans). We call this sample "location-0". The location-0 optional correction module performs the process of fitting the predicted RSS using location-0 measurements such that both the predicted and measured RSS have the same values at location-0.

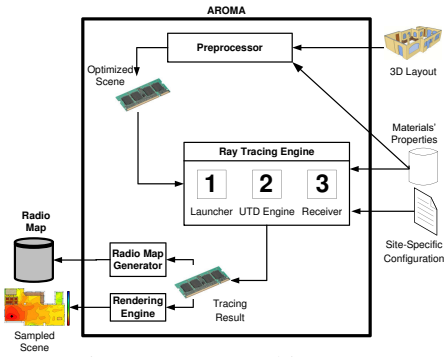

Fig. 1: System architecture.

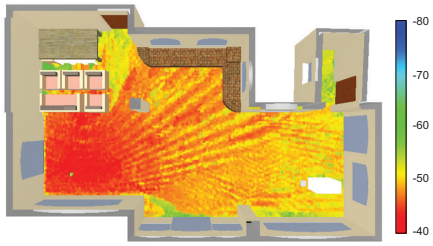

Fig. 2: An example of the output of the rendering engine.

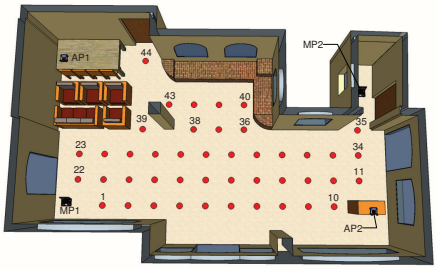

Fig. 3: Experiment layout. The figure highlights the locations of APs, MPs, and radio map locations.

E. Radio Map Generator

The results obtained from the ray tracer is processed by the *Radio Map Generator* to generate the radio map. A radio map is constructed by dividing the area of interest into a number of locations; each location has a corresponding cell in the radio map.

Our system is capable of generating two types of radio maps: **deterministic and probabilistic**. The difference between them is the type of information stored in each cell of the radio map. For a deterministic radio map, only one vector is stored in each cell representing the RSS received at the location corresponding to that cell. For a measurements-based radio map, this vector is obtained by averaging the RSS samples received from each stream over a defined time interval. Using our system, this vector is predicated by a single run of the ray tracing algorithm.

On the other hand, a probabilistic radio map requires the the knowledge of the distribution of RSS received from each stream. This information can be obtained by storing a collection of RSS samples received from different streams at each cell to predict the RSS histograms. In a measurements-based radio map, this is done by storing the RSS samples received from different streams over a defined time interval. However, the ray tracing algorithm applied in our system is deterministic and gerenates only one RSS vector for each configuration. Therefore, we applied a new approach to simulate the changes in the environment that causes the variation of the RSS. This is done by moving each device inside a 3D grid that is centered around the original location of the device. Each device location represents a new configuration and the ray tracing process is repeated for each configuration generating the samples required to predict the RSS histograms.

F. Rendering Engine

A sampled scene with RF prediction levels rendered on its floor can also be generated by processing the tracing result by the *Rendering Engine*. At the sampling step, an isotropic antenna is virtually positioned at each sampling point and the overall sampling result is then bi-cubically interpolated over the whole floor area (Fig. 2).

Transmission power (P_t)	2 mW
Antenna gain (G_{max})	3.0 dBi
Frequency (f)	2.4 GHz
Antenna type	Isotropic

TABLE I: APs' configurations.

III. System Evaluation

This section presents the experiment performed to evaluate our system. We start by describing the testbed followed by the evaluation metrics. We discuss the RSS prediction performance and the localization accuracy for both deterministic and probabilistic radio maps in Sections III-C and III-D respectively. Finally, Section III-E analyzes the effect of the model complexity on performance.

A. Testbed

Our experiment was performed in a typical apartment with an area of $700 ft^2$. The environment contained furniture and is composed of different materials like bricks, concrete, wood and glass. The layout of the experiment is shown in Fig. 3. Table I summarizes the APs' configuration used in the experiment.

We used two Cisco Aironet 1130G Series 802.11G Access Point and two D-Link DWL-G650 NICs. The system is currently implemented under the Windows OS. A NICQuery [13] driver that provides an API for user-level queries of NDIS devices is used to collect the signal strength samples. We collected 60 samples for each location in each experiment.

B. Evaluation Metrics

The following metrics are used to quantify the accuracy of the generated radio maps.

1) RSS Prediction: We used three evaluation metrics that has been used before in literature to quantify the degree of deviation of the predicated RSS from the measured one. These metrics are the Root Mean Square Error (RMSE), the Mean Absolute Error (MAE), and the Standard Deviation (Stdev).
2) Localization accuracy: We use the mean distance error between the locations estimated by the measured and generated radio maps as an estimate for the localization accuracy.

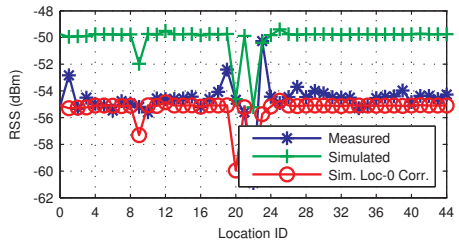

(a) RSS from AP1 by MP1

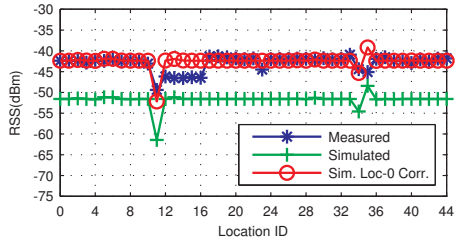

(b) RSS from AP2 by MP2

Fig. 4: Device-free experiment, measured vs. simulated RSS. Location ID refers to the IDs in Fig. 3.

C. Deterministic Radio Map Accuracy

1) RSS Prediction Performance: In this experiment, 44 locations were chosen (Fig. 3). Although, the tool can be easily used to generate radio maps with any number of humans in the area of interest, the overhead of constructing the ground truth, i.e. the measured radio map, will be prohibitive. Therefore, the experiment was performed in the presence of one human only. Measurements for location-0 are obtained during the silence period when the environment is free from any human.

Fig. 4 shows the simulated versus measured RSS for the experiment and Table II summarizes the results after using the location-0 correction module.

We show only two streams due to space constraints.

As discussed in Section II, location-0 correction is used to compensate for the constant offset between the measured and generated RSS as shown in Fig. 4. This also helps in compensating for other changes in the environment not captured by the 3D model.

The results show that simulated values are close to the measured values with a maximum average absolute error of 2.77 dB for all streams. The figure also shows that the human effect is maximum when the person is cutting the line-of-sight, e.g. locations 11, 34, and 35 in Fig. 4(b). This is captured by both the tool and the actual measurements which shows that we can use the tool to model more complex scenarios of behavior in a device-free setting.

2) Localization Performance: In this section, we compare the performance of a Mean Euclidean Distance (MED) classifier, similar to the *Radar* system [1], when trained by the measured radio map and the automatically generated one. We used 3-fold cross validation and calculated the mean distance error for both classifiers. Fig. 6 shows the CDF of distance error and Table III summarizes the results. The figure shows that,

		AP1	AP2
MP1	RMSE	1.42 dB	2.12 dB
	MAE	0.86 dB	1.56 dB
	Stdev	1.2	2.13
MP2	RMSE	3.47 dB	1.79 dB
	MAE	2.77 dB	1.07 dB
	Stdev	3.06	1.77

TABLE II: **Device-free** experiment, measured vs. simulated with **loc-0 correction**.

	Measurements	Simulation	Random (baseline)
Deterministic	1.24 m	3.13 m (10.5%)	3.46 m
Probabilistic	1.04 m	2.84 m (21.8%)	3.46 m

TABLE III: Mean distance localization error using deterministic and probabilistic radio maps. Numbers between brackets show the percentage of improvement over baseline classifier.

compared to the baseline classifier, our system can achieve more than 10% enhancement in mean distance error. This also highlights that the device-free problem is intrinsically hard and that there is still a space for improvement. The probabilistic radio map generation achieves better accuracy as we show in Section III-D2.

D. Probabilistic Radio Maps Accuracy

1) RSS Prediction Performance: In order to evaluate the effectiveness of the proposed perturbation technique proposed in Section II, we performed the two-sample KS-Test on the measured and perturbed samples. The null hypothesis was accepted for *all locations* at 0.05 significance level.

Fig. 5 shows an example of the comparison between the RSS distribution generated by devices-perturbation and that obtained by measurements at one location.

2) Localization Performance: For the localization performance, we used a Parzen windows-based classifier with Gaussian smoothing kernel.Fig. 7 shows a comparison between using measured and perturbed signals. Table III summarizes the results. The results show that, compared to the baseline classifier, our system can achieve more than 21% enhancement in mean distance error.

E. 3D Model Accuracy

Typical environments include many details that cannot be completely captured with sufficient accuracy in a 3D model either due to measurement errors or because they are hidden inside the materials. In this section, we study the effect of changing the 3D model details on accuracy. We use five models with different degrees of details: Orignal, no furniture, deformed, doors and walls only and walls only.

Fig. 8 shows the localization performance of the MED classifier for the previous models. The figure shows that adding more details to the model is not always a good thing due to the inherent errors in building materials and the location of objects. The good news is that the simplest 3D model, that only includes the walls of the area of interest, gives a very high accuracy. This can also be attributed to the use of location-0 correction model that compensates for any modeling deviations.

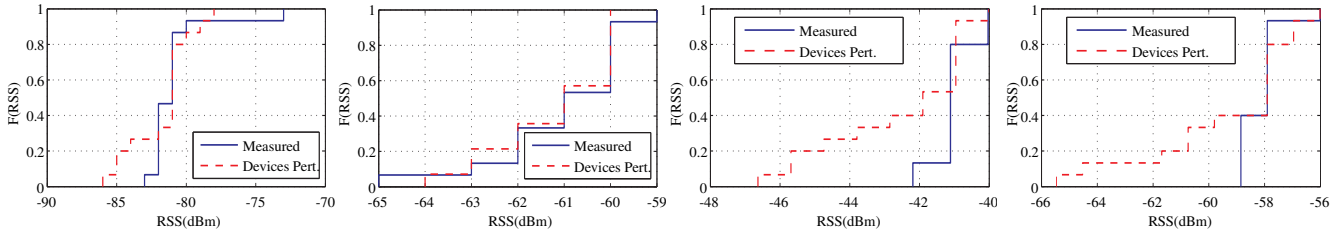

(a) Received from AP1 by MP1 (b) Received from AP1 by MP2 (c) Received from AP2 by MP1 (d) Received from AP2 by MP2

Fig. 5: CDFs of measured and perturbed signals received by each MP.

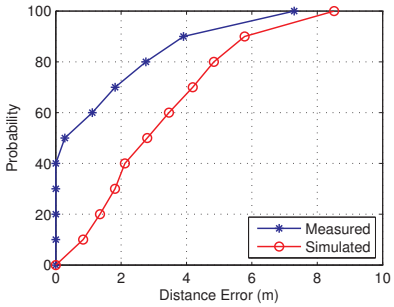

Fig. 6: Localization performance for the deterministic radio map generation.

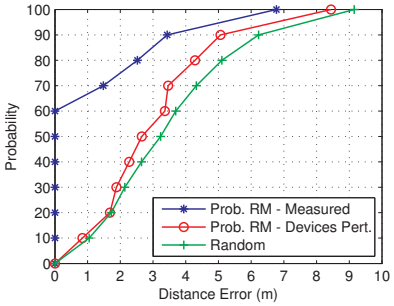

Fig. 7: Comparison of the average distance errors when using the measurements and perturbation techniques.

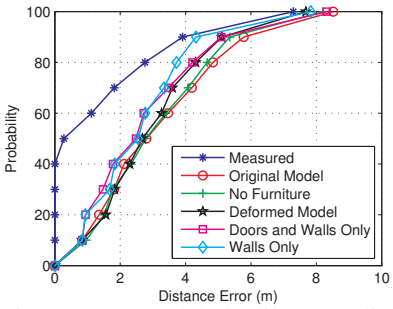

Fig. 8: 3D model details: Localization performance using measured and simulated training data using different degrees of details for the 3D model.

IV. Conclusion

This paper introduced a system capable of generating site-specific radio maps for device-free localization systems. It is also capable of constructing two types of radio maps: deterministic and probabilistic, which are used for different classes of localization systems. Our system combines 3D RF propagation with human body-scattering effects to achieve high accuracy.

The results show that high accuracy was achieved with a maximum MAE in RSS of 2.77 dB for deterministic radio maps generation. We evaluated the performance of the generated radio maps with typical localization systems. Mean distance errors of 3.13m and 2.84m were achieved using our generated deterministic and probabilistic radio maps, respectively. Our experiments have also shown that using a simple 3D model that contains only the walls of the area of interest is enough. Using the optional location-0 correction module significantly enhances results and reduces the dependence on the 3D model accuracy.

V. Acknowledgment

This work is supported in part by a grant from the Egyptian STDF.

References

[1] P. Bahl and V. N. Padmanabhan, "RADAR: An In-Building RF-based User Location and Tracking System," in *IEEE INFOCOM 2000*, vol. 2. IEEE, March 2000, pp. 775–784.

[2] M. A. Youssef and A. Agrawala, "The Horus WLAN Location Determination System," in *Communication Networks and Distributed Systems Modeling and Simulation Conference*, 2005, pp. 205–218.

[3] M. Youssef, M. Mah, and A. Agrawala, "Challenges: Device-free Passive Localization for Wireless Environments," in *MobiCom '07: Proceedings of the 13th annual ACM international conference on Mobile computing and networking*. ACM, 2007, pp. 222–229.

[4] M. Seifeldin and M. Youssef, "A deterministic large-scale device-free passive localization system for wireless environments," in *PETRA*, ser. ACM International Conference Proceeding Series, F. Makedon, Ed. ACM, 2010.

[5] A. E. Kosba, A. Abdelkader, and M. Youssef, "Analysis of a device-free passive tracking system in typical wireless environments," in *NTMS*, K. A. Agha, M. Badra, and G. B. Newby, Eds. IEEE, 2009, pp. 1–5.

[6] D. A. Mcnamara, C. W. I. Pistorius, and J. A. G. Malherbe, *Introduction to the Uniform Geometrical Theory of Diffraction*. Artech House Publishers, 1990. [Online]. Available: http://www.worldcat.org/isbn/089006301X

[7] S. Seidel and T. Rappaport, "Site-Specific Propagation Prediction for Wireless In-Building Personal Communication System Design," in *IEEE Trans. Vehicular Technology*, vol. 43, 1994, pp. 879–891.

[8] G. Athanasiadou and A. Nix, "A Novel 3-d Indoor Ray-Tracing Propagation Model : the Path Generator and Evaluation of Narrow-band and Wide-band Predictions," in *IEEE Transactions on Vehicular Technology*, vol. 49(4). IEEE, July 2000, pp. 1152–1168.

[9] Y. Ji and S. Biaz, "ARIADNE: A Dynamic Indoor Signal Map Construction and Localization System," in *in MobiSys 2006: Proceedings of the 4th international conference on Mobile systems, applications and services*. ACM Press, 2006, pp. 151–164.

[10] A. Ö. Kaya, L. J. Greenstein, D. Chizhik, R. A. Valenzuela, and N. Moayeri, "Emitter localization and visualization (ELVIS): A backward ray tracing algorithm for locating emitters," in *CISS*. Baltimore, MD, USA: IEEE, 2007, pp. 376–381.

[11] D. G., P. N., and R. T. S., "An Advanced 3d Ray Launching Method for Wireless Propagation Prediction," in *IEEE Vehicular Technology Conference 47th*, 1997.

[12] M. Ghaddar, L. Talbi, T. Denid, and A. Charbonneau, "Modeling Human Body Effects for Indoor Radio Channel using UTD," in *Electrical and Computer Engineering, 2004. Canadian Conference on*. IEEE, 2004.

[13] Microsoft, "NDISProt," Online. [Online]. Available: http://msdn.microsoft.com/en-us/library/dd163301.aspx